

Supplementary Information: Sensory stimulation enhances phantom limb perception and movement decoding

Supplementary Text

Supplementary Discussion

Supplementary Methods

Supplementary Figures

- Fig. S1. Grounding electrodes remove stimulation noise from EMG.
- Fig. S2. Prosthesis movements for movement decoding.
- Fig. S3. Long-term sensory mapping and custom socket.
- Fig. S4. Long-term movement decoding comparison across phases.
- Fig. S5. EMG decoding during sensory stimulation.
- Fig. S6. Neural recording during phantom movement and sensory stimulation.
- Fig. S7. Phantom hand movements and sensory stimulation during EEG recording.
- Fig. S8. Neural activation during phantom limb movements and sensory stimulation.

Supplementary Tables

Table S1. Participant characteristics.

Supplementary References

[49-56]

Supplementary Discussion

Sensory stimulation

Sensory feedback to the phantom hand is given using targeted transcutaneous electrical nerve stimulation (tTENS) at specific sites on the residual limb. The stimulation sites that elicit percepts in the phantom hand are generally less than 5 mm in diameter. In our experience with tTENS, the perceived activation of the phantom hand is likely not a referred sensation in the classical sense that assumes cortical takeover by neighboring regions [5]. Based on previous work, the ability to provide noninvasive sensory feedback through electrical stimulation seems to be a result of actually activating the underlying nerves and not the skin receptors in the residual limb [10, 12, 26, 11]. In our work, we believe the same mechanism is at play because sensory activation of the phantom limb does not always occur as a result of lightly touching the residual limb, which would be expected in the case of a referred sensation to the residual limb or the skin receptors; however, phantom hand activation does occur with tTENS. In fact, this same technique can be applied to intact-limb individuals to stimulate superficial nerves and elicit sensations in the hand [11]. It is unclear exactly which nerve bundles are being activated and at what level, but it is clear that we are able to achieve sensory activation of the median, ulnar, and radial regions of the phantom hand as a result of stimulating superficial nerves. For clarity, we refer to median, radial, and ulnar regions of the phantom hand as the areas traditionally innervated by the median, radial, and ulnar nerves, respectively. It should be noted that targeted sensory reinnervation (TSR), a surgical technique where sensory nerve fascicles are routed to regions away from motor nerves to enable sensory feedback, has been shown to enable haptic feedback on the skin itself to elicit sensations in the phantom hand [49]. This wouldn't be considered referred sensation in the classical sense because the underlying sensory nerves themselves are activated and give rise to the perceived phantom hand activation. Amputees with TSR can perceive phantom hand sensory activation as a result of both tTENS [26] or physical stimulation of the reinnervated sites [17, 50].

Subjective perception of enhanced control

Both the single day and the long-term experiments of this study suggest the importance of phantom limb perception on the ability to produce relevant signals for pattern recognition control of a prosthetic hand. We showed that despite no apparent physiological changes in the musculature, providing sensory stimulation to activate the phantom hand enables a greater degree of control of the phantom hand itself, both perceptually by the user as well as quantitatively through performance of the pattern recognition classifier. Subjective feedback from the amputee participants indicated stronger perception of the phantom hand as a result of sensory stimulation, which in turn enabled a greater ability to move their phantom hand despite its absence.

Previous research has shown that users tend to perceive greater embodiment of their prosthesis with somatotopically aligned sensory feedback and matched onset timing [30]. Researchers have also shown synchronous visual and tactile feedback can improve embodiment and reduce abnormal phantom limb perceptions of telescoping in an immersive virtual reality environment [51]. Our experiments were not designed to capture changes in prosthesis embodiment or agency, but we did see that sensory stimulation induced a heightened perception of the phantom hand in every case. We postulate that in order to create a lifelike prosthesis, it is necessary to develop methods for strengthening the internal sensorimotor models of the amputee's phantom hand. The phantom hand sensation should be utilized in a way that can improve prosthesis control, which in turn will hopefully lead to even better device embodiment by the user. We have shown that sensory stimulation to peripheral nerves improves perceptions of the phantom hand, which in turn improves the ability to generate consistent myoelectric signals for pattern recognition. The sensory stimulation likely does not change the physiological nature of the amputated limb, yet tTENS seems to be a factor in the ability to reliably produce voluntary muscle contractions in the residual limb making complex movements with the phantom hand.

Supplementary Methods

Sensory map similarity

The structural similarity (SSIM) index [31] was used to compare similarity of sensory mapping regions of the phantom hand across different days. We cropped each sensory mapping image to the region of interest (median, ulnar, or radial) and removed the background so that only the colored regions remained. We used the SSIM function in MATLAB (Mathworks, Natick, USA) and compared each sensory mapping image to all other images with the same region of interest. This was done for every image and the results were averaged together to generate a single value for each day (Fig. 4B). To calculate the sensory coverage area (Fig. S3A), we removed the background from every sensory mapping image and converted the image to grayscale. The percentage area was calculated by summing the number of elements with color and dividing by the total number of elements in the image of the hand.

EMG features

Features of the EMG signals were extracted using a 200 ms sliding window with new feature vectors computed every 50 ms. The EMG signal features used were mean absolute value (MAV) (Eq. 1), waveform length (WL) (Eq. 2), and variance (VAR) (Eq. 3)

$$MAV = \frac{1}{N} \sum_{k=1}^N |x_k| \quad (1)$$

$$WL = \sum_{k=2}^N |x_k - x_{k-1}| \quad (2)$$

$$VAR = \frac{1}{N} \sum_{k=1}^N (x_k - \mu)^2 \quad (3)$$

N is the number of samples, x_k is the k^{th} sample, and μ is the mean of x . We performed min-max feature scaling on the training data and applied the same scale to the testing data. These time domain (TD) features and methods are commonly used for pattern recognition with EMG signals [52, 53].

EEG site classification

For classifying the stimulation site from neural activity (Fig. S6), multi-class spatial patterns (CSP) [54] were used as features in a 100 ms sliding window for a support vector machine (SVM) classifier. We used a data holdout strategy with 80% for training and 20% for testing the classification. A sequential feature selection algorithm (SFFS) [55] was used to select a subset of features. A grid search was performed to select the optimal hyper parameters for the SVM classifier. Processing was done using the gumpy Python toolbox [56].

Stimulation noise removal

During the experiment with simultaneous tTENS and EMG recording with A02, a band of earth grounded electrodes (Ag/AgCl, Nortrode 20, Myotronics, USA) was placed on A02's residual limb in between the site of stimulation and the EMG recording electrodes. To evaluate the ability of the grounding electrodes to remove stimulation artifact from the EMG signal, we performed simultaneous tTENS and EMG recording on the left arm of an able-bodied subject. The stimulation site was located above the median nerve at the wrist on the ventral side of the forearm (Fig. S1A). The tTENS reference electrode was placed on the back of the left thumb. The area of perceived activation was on the palmar side of the thumb. Grounding electrodes were placed approximately 10 cm proximal to the stimulation site, and 8 EMG electrodes (13E200 Myobock amplifiers, Ottobock, Plymouth, MN) were located approximately another 5-10 cm proximal along the forearm. Stimulation was applied at 0.4 mA at either 2 Hz or 40 Hz. EMG was recorded at rest (no movement), during stimulation without the grounding electrodes, and again during stimulation with grounding electrodes. Signals were recorded by an NI USB-6009 (National Instruments, Austin, TX) at 1024 Hz with 20 – 500 Hz digital bandpass and 60 Hz notch filters. The filtered EMG signal showed significant noise artifact as a result of stimulation, but this artifact was removed from the EMG waveform by the grounding electrodes (Fig. S1B-D).

Table S1. Participant characteristics.

(A) Details on the amputee volunteers and their myoelectric pattern recognition and prosthesis control experience.

Participant	Age (yr)	Amputation	Cause	Time of Amputation	Prosthesis	Experience
A01	39	left, transhumeral	brachial plexus injury resulting in paralysis of the arm	nerve injury Jan. 2018, elective amputation March 2018	no prosthesis	no myoelectric control experience
A02	49	right, transradial	compartment syndrome resulting in paralysis of the arm	nerve injury 2002, elective amputation Nov. 2017	prosthesis, direct myoelectric control	1 month of EMG pattern recognition experience
A03	29	left, transhumeral right, transradial	septicemia resulting from meningitis	Oct. 2010	left arm prosthesis, pattern recognition control	5 years of myoelectric direct control and 1 year of EMG pattern recognition experience
A04	64	left, transhumeral, targeted muscle reinnervation (TMR)	disease in forearm	2007, TMR 2012, osseointegration 2015	prosthesis, pattern recognition control	>8 years of pattern recognition experience

(B) Amputee participation across experiments.

Participant	Sensory Mapping	User Survey	Movement Decoding	Long-Term Study	Movement During TENS	Object Movement Task	EEG Recording
A01	X	X	X				
A02	X	X	X		X		X
A03	X	X	X	X			X
A04	X					X	

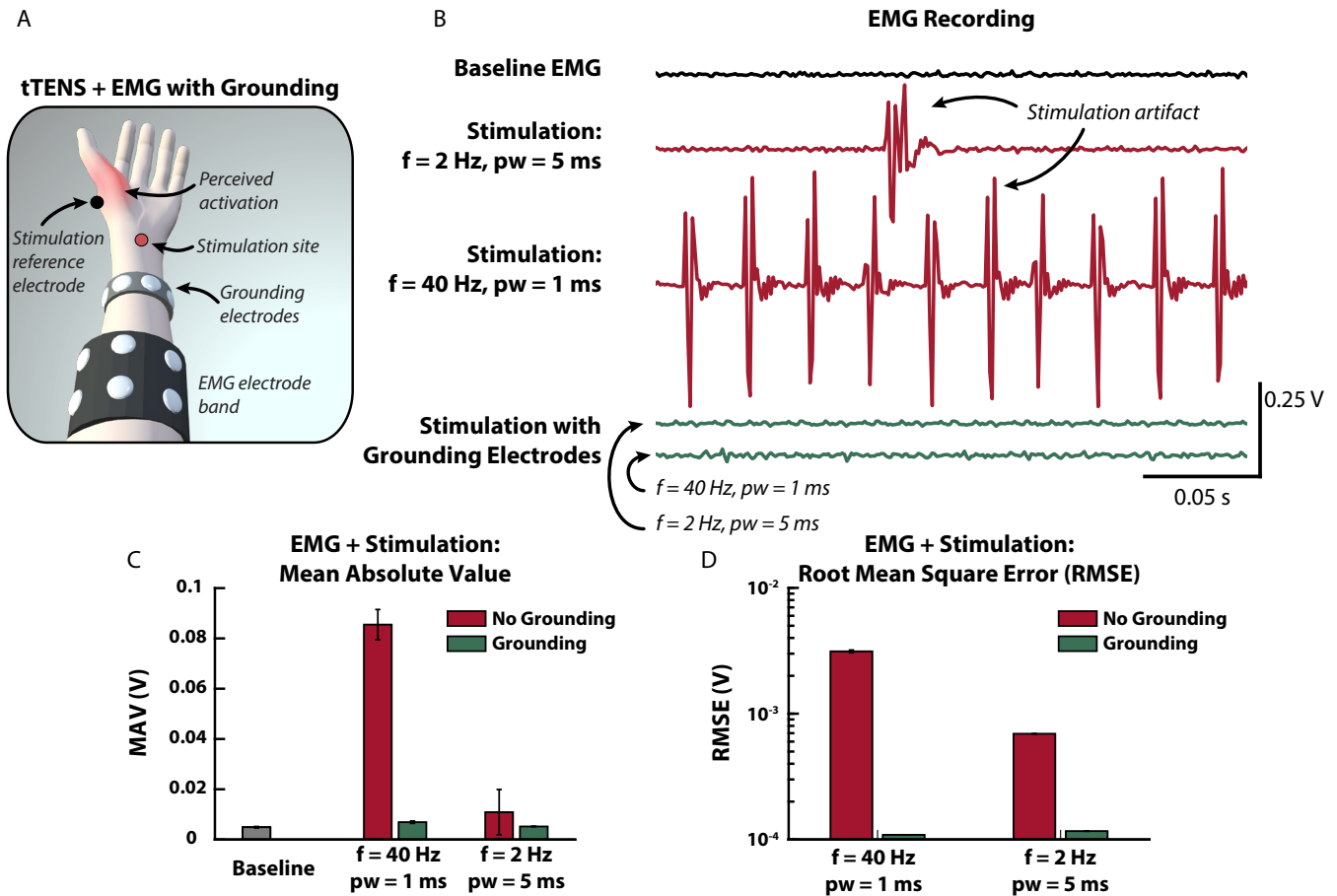


Fig. S1. Grounding electrodes remove stimulation noise from EMG. (A) To make sure that the tTENS signal was not affecting the EMG recording, we placed a band of earth grounded electrodes in between the stimulation and EMG recording sites in an able-bodied subject (*SI Methods: Stimulation noise removal*). For this subject, the perceived area of activation was in the thumb region. (B) During stimulation at both low (2 Hz) and high (40 Hz) frequencies, significant artifact is present in the EMG signal during no movement (red traces). These traces show actual EMG recording from the most adversely affected EMG electrode during tTENS. By placing the grounding electrodes on the arm, the stimulation artifact is effectively removed (green traces). (C) The mean absolute value (MAV) of the EMG signal is increased during stimulation without grounding hardware. The addition of grounding electrodes removes noise effects in the EMG signal. (D) The root mean square error (RMSE) was calculated between the FFT of the EMG signal during tTENS and the baseline EMG signal. Bars represent the standard deviation. The presence of grounding hardware greatly reduces the RMSE.

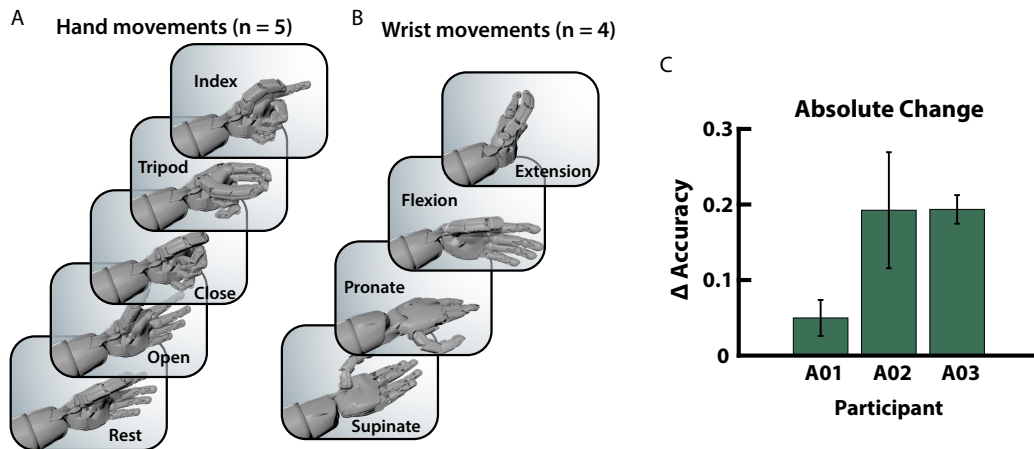


Fig. S2. Prosthesis movements for movement decoding. (A) Five hand and (B) four wrist movements were presented as visual cues during the EMG recording. The amputees matched the movements with their phantom hand while EMG signals were recorded from the residual limb. (C) Absolute change in movement decoding performance after sensory stimulation to the phantom hand. N=3 per bar.

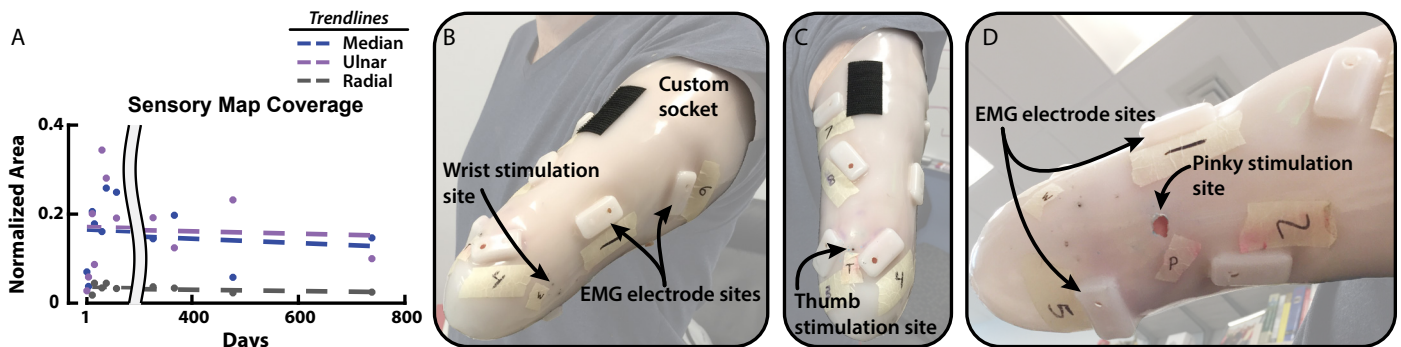


Fig. S3. Long-term sensory mapping and custom socket. (A) The long-term sensory coverage area for each region (median, ulnar, and radial) to the area of the entire hand. The normalized area is calculated by comparing the area of coverage of each region (median, ulnar, and radial) to the area of the entire hand. (B) To ensure repeatable EMG electrode placement, a custom socket was used for amputee A03 during data collection. Eight electrodes were positioned by a prosthetist to optimize muscle coverage in the residual limb. Small holes were created in the socket for the stimulating probe to activate (A) wrist, (B) thumb, and (C) pinky regions of the phantom limb through tENS.

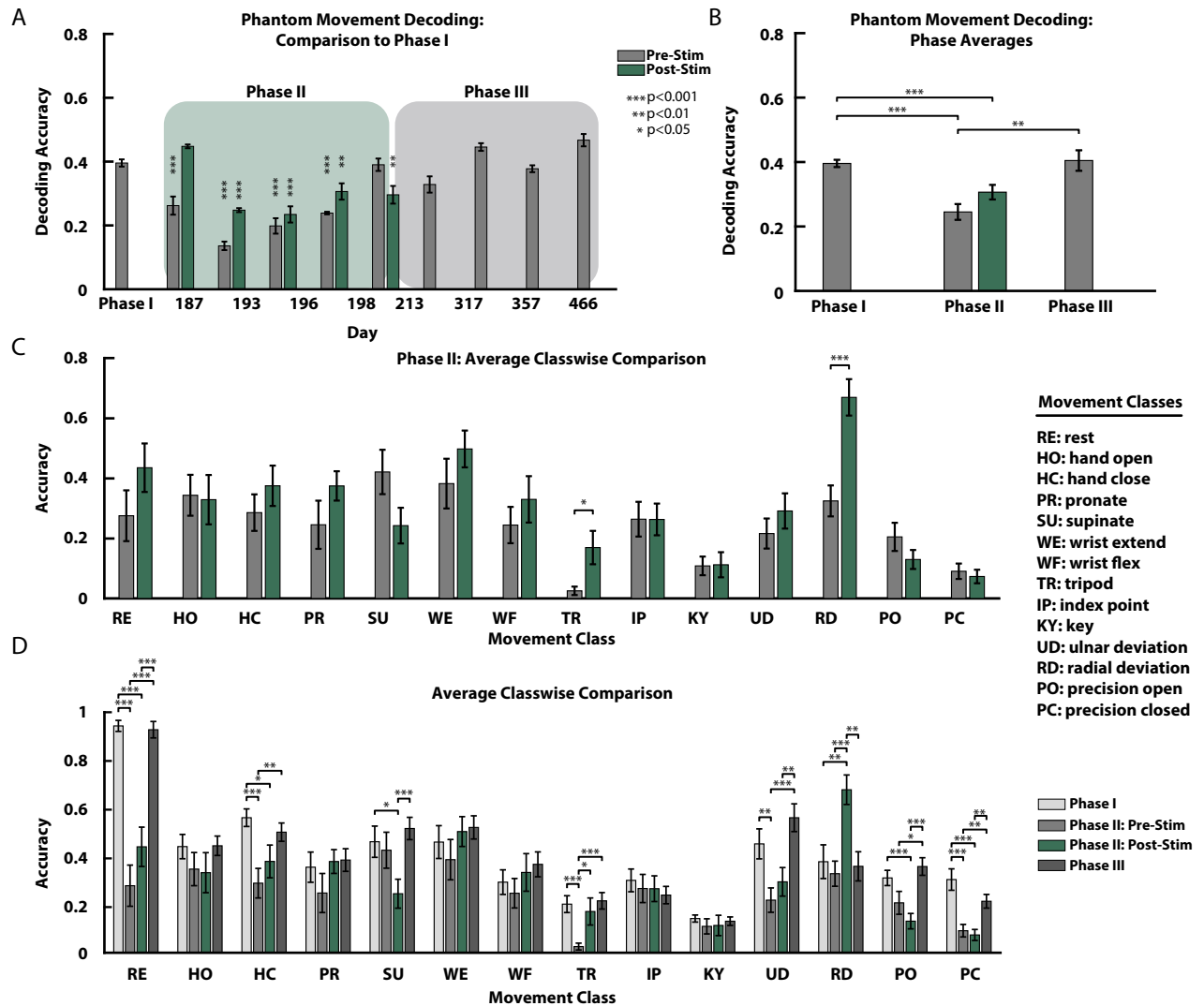


Fig. S4. Long-term movement decoding comparison across phases. (A) Phase I ($n=18$) compared to individual days in Phase II and III ($n=3$ for each bar) shows only major differences ($p < 0.05$) to performance in most days in Phase II but not for any day in Phase III. (B) The average movement decoding performance for Phase I ($n=18$), Phase II ($n=12$ for each group), and Phase III ($n=12$). Phase II performance, both Pre-Stim and Post-Stim, is lower compared to Phases I and III ($p < 0.01$). There were no apparent major differences ($p > 0.05$) between Phases I and III, despite the observed slight increasing trend over the course of Phase III. The benefit from tTENS appears to be short-term (i.e. within the same day) and any long-term improvement is likely due to continued prosthesis use by participant.

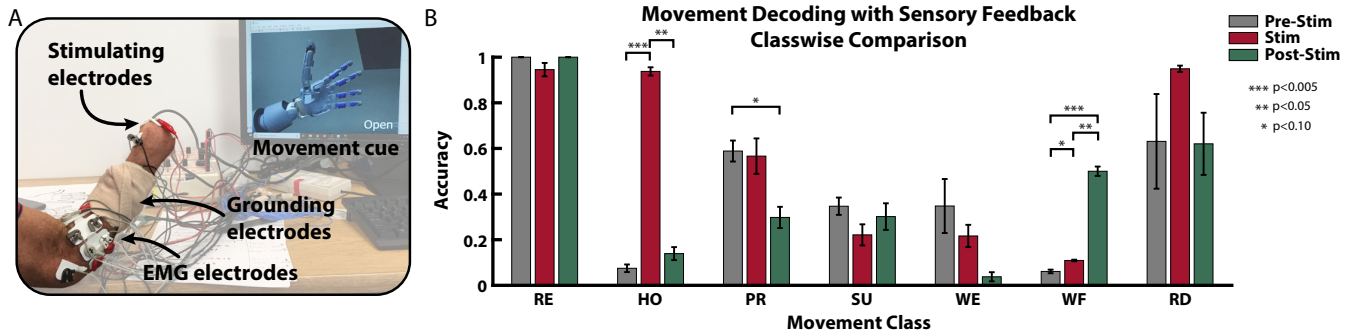


Fig. S5. EMG decoding during sensory stimulation. (A) EMG electrodes were placed on the forearm and tTENS electrodes were placed at the distal end of the residual limb. A set of grounding electrodes were placed between the stimulating and EMG recording electrodes to prevent stimulation noise in the myoelectric signal (Supplementary Methods, Supplementary Fig. S1). Movement cues were displayed on a screen (Movie S2). (B) Overall, decoding performance improves during trials with sensory stimulation. Movement classes are RE: rest, HO: hand open, PR/SU: wrist pronate/supinate, WE/WF: wrist extension/flexion, and RD: radial deviation. Specific classes appear to benefit from sensory stimulation to the phantom hand, specifically hand open, wrist flexion, and radial deviation. Antagonistic movements, specifically wrist extension appears to be negatively influenced. $N = 3$ per bar.

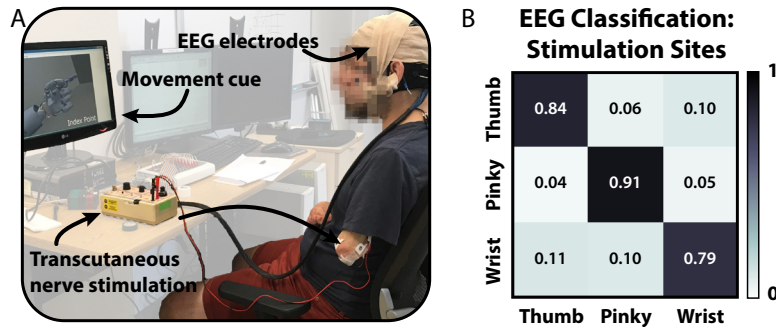


Fig. S6. Neural recording during phantom movement and sensory stimulation. (A) Patient A03 was shown movement cues during EEG recordings. Targeted transcutaneous electrical nerve stimulation (tTENS) was used to provide sensory stimulation to the phantom hand during movements. Neural signals from trials with and without sensory stimulation were recorded. (B) Using SVM, the stimulation region can be classified from the neural signal (Supplementary Methods).

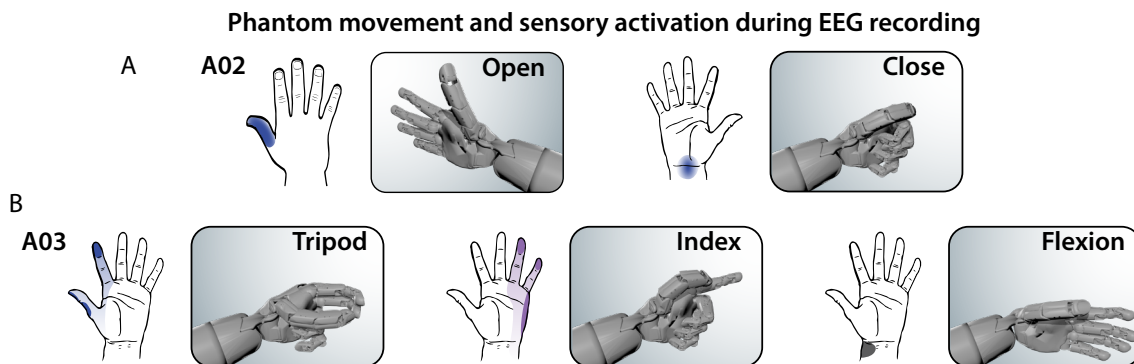


Fig. S7. Phantom hand movements and sensory stimulation during EEG recording. (A) Patient A02 was stimulated in the thumb of the phantom hand during hand open movements. During hand close, he was stimulated in the wrist region. These locations were chosen for A02 based on recommendations from the participant as to what parts of his phantom hand that could be stimulated and that he was focusing on for hand open and close. (B) For A03, sensory activation of the thumb and index fingers was provided during the tripod grasp movement. The pinky of the phantom hand was activated during index point, and the wrist was stimulated during wrist flexion. The sensory stimulation locations for A03 were chosen based on the movements and stimulation regions identified for the long-term study.

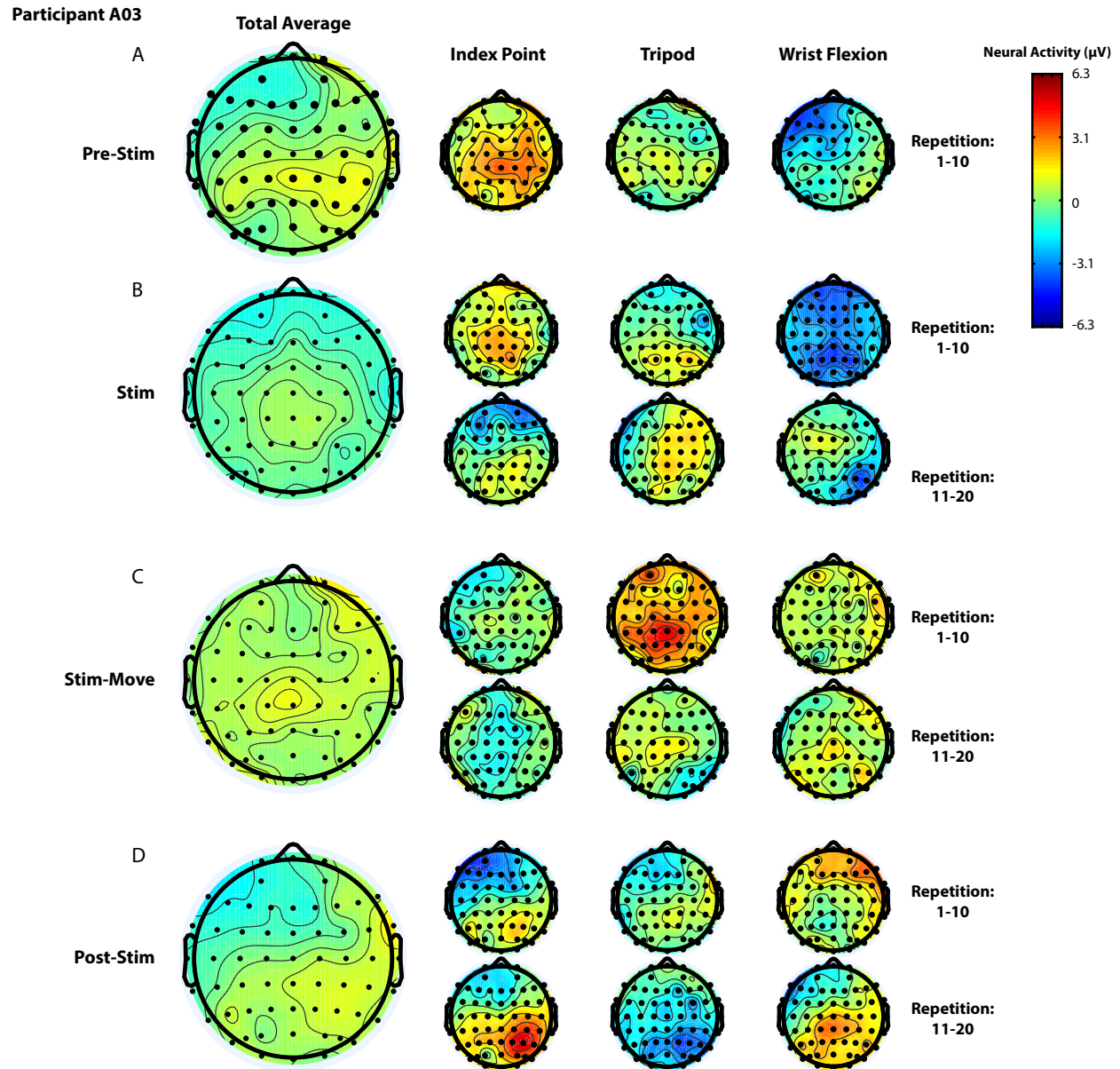


Fig. S8. Neural activation during phantom limb movements and sensory stimulation. (A) EEG signals from amputee A03 were recorded during phantom hand movements before any stimulation (Pre-Stim), (B) during sensory stimulation but with no movement (Stim), (C) sensory stimulation during phantom hand movement (Stim-Move), and (D) movements after sensory stimulation (Post-Stim). Averages of 10 repetitions of each movement (index point, tripod, and wrist flexion) are shown in the small EEG maps for each condition. The total average from all repetitions are shown in the by the larger EEG activity maps on the left.